

Mobility edges in one-dimensional finite-sized models with large quasi-periodic disorders

Qiyun Tang(汤起芸) and Yan He(贺言)
Citation: Chin. Phys. B, 2023, 32 (**12**): 127202. DOI: 10.1088/1674-1056/accdc9
Journal homepage: http://cpb.iphy.ac.cn; http://iopscience.iop.org/cpb

What follows is a list of articles you may be interested in

General mapping of one-dimensional non-Hermitian mosaic models to non-mosaic counterparts: Mobility edges and Lyapunov exponents

Sheng-Lian Jiang(蒋盛莲), Yanxia Liu(刘彦霞), and Li-Jun Lang(郎利君)
Chin. Phys. B, 2023, 32 (**9**): 097204. DOI: 10.1088/1674-1056/ace426

Mobility edges and reentrant localization in one-dimensional dimerized non-Hermitian quasiperiodic lattice

Xiang-Ping Jiang(蒋相平), Yi Qiao(乔艺), and Jun-Peng Cao(曹俊鹏)
Chin. Phys. B, 2021, 30 (**9**): 097202. DOI: 10.1088/1674-1056/ac11e5

Uncertainties of clock and shift operators for an electron in one-dimensional nonuniform lattice systems

Long-Yan Gong(巩龙延), You-Gen Ding(丁友根), Yong-Qiang Deng(邓永强)
Chin. Phys. B, 2017, 26 (**11**): 117201. DOI: 10.1088/1674-1056/26/11/117201

Phase diagram of a family of one-dimensional nearest-neighbor tight-binding models with an exact mobility edge

Long-Yan Gong(巩龙延), Xiao-Xin Zhao(赵小新)
Chin. Phys. B, 2017, 26 (**7**): 077202. DOI: 10.1088/1674-1056/26/7/077202

Thermoelectric properties of $Sr_{0.61}Ba_{0.39}Nb_2O_{6-\delta}$ ceramics in different oxygen-reduction conditions

Li Yi (李宜), Liu Jian (刘剑), Wang Chun-Lei (王春雷), Su Wen-Bin (苏文斌), Zhu Yuan-Hu (祝元虎), Li Ji-Chao (李吉超), Mei Liang-Mo (梅良模)
Chin. Phys. B, 2015, 24 (**4**): 047201. DOI: 10.1088/1674-1056/24/4/047201

Mobility edges in one-dimensional finite-sized models with large quasi-periodic disorders

Qiyun Tang(汤起芸) and Yan He(贺言)[†]

College of Physics, Sichuan University, Chengdu 610064, *China*

(Received 7 March 2023; revised manuscript received 13 April 2023; accepted manuscript online 18 April 2023)

We study the one-dimensional tight-binding model with quasi-periodic disorders, where the quasi-period is tuned to be large compared to the system size. It is found that this type of model with large quasi-periodic disorders can also support the mobility edges, which is very similar to the models with slowly varying quasi-periodic disorders. The energy-matching method is employed to determine the locations of mobility edges in both types of models. These results of mobility edges are verified by numerical calculations in various examples. We also provide qualitative arguments to support the fact that large quasi-periodic disorders will lead to the existence of mobility edges.

Keywords: quasi-periodic disorders, mobility edges, Aubry–Andre model

PACS: 72.20.Ee, 71.23.–k **DOI:** 10.1088/1674-1056/accdc9

1. Introduction

The phenomena of localization[1] have been extensively studied in condensed matter physics for many years. For three-dimensional (3D) systems, a threshold of disorder strength exists, above which the Anderson localization will take place. For generic band structures, a closely related notion is the mobility edge[2] which is the critical energy separating the localized and extended energy eigenstates. Since the direct observation of mobility edges in a 3D system is quite challenging, attention has been turned to low-dimensional systems. However, the number of dimensions is a very important factor for Anderson localization. It is argued by the scaling theory[3,4] that for one-dimensional (1D) systems even infinitesimal small disorders will make all eigenstates completely localized. Thus, one cannot find any mobility edges in the 1D band structure.

About forty years ago, the low-dimensional quasi-periodic systems with correlated disorders were proposed and captured a lot of attention. The most famous example is the so-called Aubry–Andre (AA) model.[5,6] In essence, the AA model is just a 1D tight-binding model with incommensurate or quasi-periodic on-site potentials. By Fourier transformation, one can show that the hopping terms and potential terms of the AA model can transfer into each other. By equating the hopping terms with the potential terms, one can see that a self-dual symmetry exists in the AA model. It is easy to see that this self-dual point will separate between the localized and extended states. Unfortunately, one still cannot find any mobility edges in the standard AA model.

In order to make mobility edges possible in the AA-type models, Das Sarma and co-workers[7–9] introduce the slowly varying quasi-periodic potentials into the AA model. This new class of 1D model was shown to support the mobility edges and has been extensively studied ever since. The success of slowly varying quasi-periodic model stimulated a lot of more works on the mobility edges in 1D quasi-periodic systems.[10–13] It is also found that the mobility edge can appear in many different types of modified AA model such as in Refs. [14–19]. During the same time, the mobility edges of many different models have been studied.[20–23] A variety of novel physical phenomena induced by the mobility edge and methods to determine the mobility edges are also explored extensively.[24–30] In addition, the research of mobility edge has been further extended to the domain of non-Hermitian systems.[31–37]

In this paper, we present another version of modified AA model, which can also accommodate mobility edges. In this modified AA model, we simply replace the irrational frequency α with another much smaller irrational frequency such as α/M where $M \sim 10^2$. Due to this much smaller irrational frequency, our model has a quite long quasi-period, which is roughly a few percent of the system size. Here we emphasize that the system size must be kept finite. We will call this model the "AA model with large quasi-periodic disorders". We will present a detailed study of mobility edges of this large quasi-periodic model with disorders in on-site potentials or in hopping coefficients or in both. We will see that, in each case, their mobility edges are very similar to the AA model with slow-varying quasi-periodic disorders.

We can determine the location of these mobility edges by the so-called energy-matching method that we have proposed in our previous works.[38] In essence, we can approximate the above quasi-periodic disordered model by an ensemble of different periodic models. Then the region of extended states can be approximately obtained by the overlaps of energy bands of

[†]Corresponding author. E-mail: heyan_ctp@scu.edu.cn

© 2023 Chinese Physical Society and IOP Publishing Ltd

all these periodic models. We will demonstrate this method works quite efficiently in determining the mobility edges for different versions of AA models with large quasi-periodic disorders. In the end of this paper, we will present qualitative arguments in support of the existence of mobility edges in the models with large quasi-periodic disorders.

The rest of this paper is organized as follows. In Section 2, we introduce the two types of quasi-periodic disordered models, which will be studied closely. Then we present a brief review of the energy matching method in Section 3. In Section 4, we will apply this method to determine the mobility edges of various disordered models and also use detailed numerical calculations to verify them. In Section 5, we provide a qualitative explanation of the existence of mobility edges in large quasi-periodic disordered models. At last, we briefly conclude in Section 6.

2. The large quasi-period disordered model and slowly varying disordered model

In this paper, we will mainly focus on the modified AA models with very small irrational frequencies or large quasi-periodic disorders. The Hamiltonian of this type of models can be summarized as

$$\hat{H} = -\sum_{i=1}^{N-1}(t+w_i)(\hat{c}_i^{\dagger}\hat{c}_{i+1}+\hat{c}_{i+1}^{\dagger}\hat{c}_i)+\sum_{i=1}^{N}\mu_i\hat{c}_i^{\dagger}\hat{c}_i, \tag{1}$$

here $\hat{c}_i$ ($\hat{c}_i^{\dagger}$) is the fermionic annihilation (creation) operator, N is the total number of lattice sites. For convenience, we set $t=1$ as the energy unit. Disorders with large quasi-periods are introduced into the above model by the following assumptions:

$$w_i = w\cos\left(2\pi\frac{\alpha}{M}i\right),\ \ \mu_i = \mu\cos\left(2\pi\frac{\beta}{M}i+\phi\right). \tag{2}$$

Here w and μ are the amplitude of the disorder and i labels the lattice site. α and β are certain order 1 irrational numbers, which determine the quasi-periodic behavior. In particular, if one set $\alpha=0$, then the model only contains disorders in potential terms. Similarly, one can also put the disorders in the hopping term or in both hopping and potential terms. Here ϕ is some fixed phase angle, which can tune the relative disorder between the potential terms and hopping terms. Most importantly, we also introduce a large integer M in the denominators, which is used to control the order of magnitude of irrational frequencies. It is easy to see that the length of quasi-period of w_i and μ_i is given by

$$T_\alpha = \frac{M}{\alpha},\ \ T_\beta = \frac{M}{\beta}, \tag{3}$$

which is quite long when compared to the system size. In this sense, we call it the long quasi-period model.

Throughout the whole paper, we will often compare the models of large quasi-periods disorders with the models of slowly varying quasi-periodic disorders. As we discussed in the introduction, the model with slowly varying quasi-period is well known to support the mobility edges. Its Hamiltonian can be expressed as

$$\hat{H} = -\sum_{i=1}^{N-1}(t+w_i')(\hat{c}_i^{\dagger}\hat{c}_{i+1}+\hat{c}_{i+1}^{\dagger}\hat{c}_i)+\sum_{i=1}^{N}\mu_i'\hat{c}_i^{\dagger}\hat{c}_i, \tag{4}$$

where

$$w_i' = w'\cos(2\pi\alpha i^{v}),\ \ \mu_i' = \mu'\cos(2\pi\beta i^{v}+\phi). \tag{5}$$

One usually assumes the exponent v to satisfy $0<v<1$. In this case, one can see both w_i' and μ_i' approaches to some constant value as i become very large. This behavior justifies the name of slowly varying quasi-period disorders.

Due to the characteristic that w_i' and μ_i' approach constants in the large i limit, one can give a heuristic argument to determine the mobility edge of the slowly varying quasi-periodic model in certain cases. In this method, the asymptotic constancy of w_i' and μ_i' is considered to be an important condition for the generation of mobility edges. The large quasi-periodic model does not have this property that disorders gradually approaching constants, but it still produces mobility edges similar to the slowly varying quasi-periodic models. This shows that the asymptotic constancy of w_i' and μ_i' is not a necessary condition for the existence of mobility edges.

There is a simple physical picture that can roughly explain why the mobility edges can exist in the slowly varying disordered models. For small i, the model of Eq. (4) will favor the localized states due to the disorders. On the other hand, for large i, the model of Eq. (4) becomes uniform and favors the extended state. It is the competition of these two effects that gives rise to the mobility edges in the slowly varying disordered models. In Section 5, we will provide some simple arguments to explain the appearance of mobility edges in the large quasi-periodic disordered models.

In the rest of this paper, we will set the irrational number α or β in the above two types of models to be $\frac{\sqrt{5}-1}{2}$. The total number of lattice sites is set to be $N=10000$.

3. Introducing the energy-matching method

The "energy-matching method" is an effective method to determine the mobility edge. The basic idea of this method is to approximate the quasi-periodic disordered models by an ensemble of periodic models. For convenience, we label these periodic models by $a=1,\ldots,N$. Then their Hamiltonian can be written as

$$\hat{H}_a = -\sum_{i=1}^{N}(t+w_a)(\hat{c}_i^{\dagger}\hat{c}_{i+1}+\hat{c}_{i+1}^{\dagger}\hat{c}_i)+\sum_{i=1}^{N}\mu_a\hat{c}_i^{\dagger}\hat{c}_i,$$

$$w_a = w\cos\left(2\pi\frac{\alpha}{M}a\right),\ \ \mu_a = \mu\cos\left(2\pi\frac{\beta}{M}a+\phi\right). \quad (6)$$

Here periodic boundary conditions such as $c_{N+1} = c_1$ are imposed and w_a and μ_a do not depend on the lattice site. For each $\hat{H}_a$, we can diagonalize the Hamiltonian in the momentum space to find the extended eigenstates with the following energy bands:

$$E = \mu_a - 2(t+w_a)\cos k. \quad (7)$$

Although we cannot diagonalize the quasi-periodic disordered model analytically, one can expect intuitively that the eigenstate of a given energy E is extended, if this energy E is located inside in the energy band of all the periodic model $\hat{H}_a$. Therefore, the energy region of the extended state of the model of Eq. (1) will be the overlap of all energy bands of Eq. (7)

$$E \in \bigcap_a \Big(\mu_a - 2(t+w_a), \mu_a + 2(t+w_a)\Big). \quad (8)$$

The energy-matching method can also be applied to the model with slowly varying quasi-periodic disorders. In this case, one only needs to change w_a and μ_a to the following

$$w_a = w\cos(2\pi\alpha a^v),\ \ \mu_a = \mu\cos(2\pi\beta a^v+\phi). \quad (9)$$

In a previous paper,[38] we have verified that the energy-matching method can give the correct location of mobility edges in this case.

In the next section, we will apply this method to calculate the mobility edges of the models with large quasi-period and the models with slowly varying disorders in several different examples. We will verify that the numerical results of mobility edges are consistent with the result of energy-matching method. In the meantime, the above two types of models will give rise to the same mobility edges.

4. Numerical verification of mobility edges

In this section, we choose the inverse participation ratio (IPR) and Lyapunov exponent,[39–41] which are common physical quantities of disordered systems, as the indicators to distinguish between extended states and localized states. These indicators can help us to numerically verify the accuracy of the mobility edges, which are obtained by the energy-matching method in the previous section.

The inverse participation ratio (IPR) of the n-th normalized eigen-wave function ψ_n is defined as

$$\mathrm{IPR}_n = \sum_{j=1}^{N}\left|a_j^n\right|^4,\ \ \psi_n = (a_1^n,\ldots,a_N^n). \quad (10)$$

For the extended states, one expects that their amplitudes are roughly uniform. Thus each component of ψ_n is roughly the same order of magnitude $|a_j^n| \sim 1/N$ for all j. Then it is easy to see that the IPR of the extended state should be the order of $\sum_{j=1}^{N}\frac{1}{N^2} = \frac{1}{N}$, which approaches 0 as the system size $N \to \infty$. On the other hand, the non-zero amplitudes of localized states will mostly confined to only a few components. Therefore, in this case, we expect the IPR to be order 1.

At the same time, one can also calculate the Lyapunov exponent of the system, which is defined as

$$\gamma(E_u) = \frac{1}{N-1}\sum_{u\neq v}^{N}\ln|E_u - E_v| - \frac{1}{N-1}\sum_{i}^{N-1}\ln|t+w_i|. \quad (11)$$

It is well-known that the Lyapunov exponent is the inverse of the localization length. Therefore, one expects the non-zero Lyapunov exponent $\gamma \neq 0$ for localized states. On the other hand, the Lyapunov exponent will be almost zero for extended states.

4.1. The AA model with disordered potential

As the first example, we consider the case with $\alpha = 0$ and $\beta = (\sqrt{5}-1)/2$, which means the disorders are only in the potential. This is also the original version of the AA model. In this case, w_a is just a constant w. According to energy-matching method, the lower bound of the region of extended states is determined by the maximum value of the bottom of each energy band of $\hat{H}_a$, which can be denoted as $E_{\mathrm{bottom}} = \mu_a - 2(t+w)$. Similarly, the upper bound of extended states is determined by the minimum value of the top of each energy band of $\hat{H}_a$, which is $E_{\mathrm{top}} = \mu_a + 2(t+w)$. It is easy to see that the resulting energy region of extended states is

$$E \in \Big(\mu - 2(t+w), -\mu + 2(t+w)\Big). \quad (12)$$

As μ is tuned, the above upper and lower bounds generate two lines of mobility edges separating extended states from localized states.

To verify the above mobility edges, we plot the eigenenergy of the AA model with large quasi-period disordered potential of Eq. (1) as a function of μ in Fig. 1(a). The parameters used in this calculation are listed in the figure caption. The color of each point represents the IPR value of the eigenstates. One can see that the boundary of the dark region matches the mobility edges that we have decided above by the energy-matching method. Similarly, we plot the eigenenergy of the slowly varying AA model Eq. (4) with disordered potential in Fig. 1(b). The parameters of α, β in the slowly varying AA model are the same as those in the AA model with the large quasi-period. We also assume $w' = w$ and the slowly varying exponent as $v = 0.5$. It can be seen from the figure that the mobility edges of the two types of models are the same, and they are both consistent with the calculated results of Eq. (12).

In order to make more quantitative observations, in Figs. 1(c)–1(f), we also plot the IPR values and Lyapunov exponent as a function of eigenenrgy for a few selected points as

$\mu = 0.9, 1.6, 2.5$. While figures 1(c) and 1(d) show the results of the AA model with a large quasi-period, and figures 1(e) and 1(f) show the results of slowly-varying AA model. One can see that the IPR drops from the order of magnitude of 10^{-2} to 10^{-4} when the eigenenergy across certain critical values, and the Lyapunov exponent will also change from non-zero to zero. This clearly signals the transition from localized states to extended states. These figures also support the conclusion that the mobility edges of the two types of models are both consistent with formula (12).

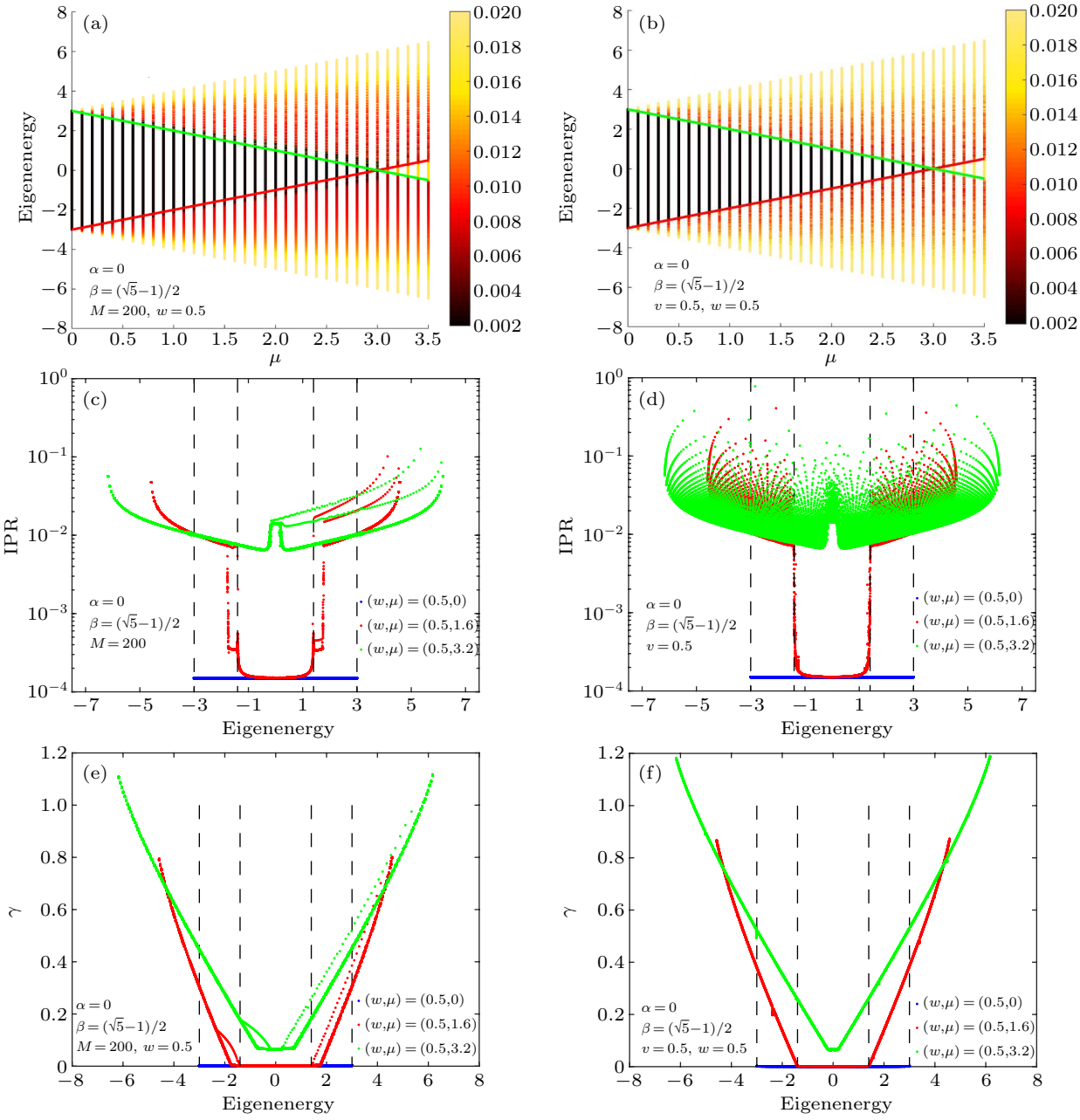


Fig. 1. (a) Eigenenergy of the model of Eq. (1) as a function of μ with $\alpha = 0$, $\beta = (\sqrt{5}-1)/2$, $w = 0.5$ and $M = 200$. (b) Eigenenergy of the model of Eq. (4) as a function of μ' with $w' = w$ and $v = 0.5$, other parameters are the same as (a). The colors in panels (a) and (b) represent the IPR of each eigenstate. The red and green curves represent the mobility edges. (c) and (e) The IPR and Lyapunov exponent of Eq. (1) as a function of eigenenergy for $(w,\mu) = (0.5,0), (0.5,1.6), (0.5,3.2)$, other parameters are the same as (a). (d) and (f) The IPR and Lyapunov exponent of Eq. (4) with $w' = w$ and $v = 0.5$, other parameters are the same as (c).

4.2. The AA model with the same disorders in hopping and potential

Now we turn to a more complicated model with $\beta = \alpha$ and $\phi = 0$. In this case, μ_i and w_i have the same disorder. For this model, we can also use the energy-matching method to determine the mobility edge. The lower bound of the energy region of Eq. (8) is determined by the extreme values $E = \mu - 2(t+w)$ and $E = -\mu - 2(t-w)$. Depending on the value of μ, we will take the larger one as the lower bound. When $\mu > 2w$, clearly, the lower bound of the energy region of the extended state is $E_{\min} = \mu - 2(t+w)$. One the other hand, if $\mu < 2w$, we have $E_{\min} = -\mu - 2(t-w)$ as the lower

bound.

Similarly, we can also get extreme values $E=\mu+2(t+w)$ and $E=-\mu+2(t-w)$ for the upper bound of the energy region of the extended state. Obviously, regardless of the value of μ and w, the energy $E=-\mu+2(t-w)$ is smaller. So the upper bound of the energy region of the extended states is $E_{\max}=-\mu+2(t-w)$. In summary, when $\beta=\alpha$, we find the condition for extended states is given by

$$E\in\Big(-\mu-2(t-w),-\mu+2(t-w)\Big),\quad \text{for } 0<\mu<2w,$$
$$E\in\Big(\mu-2(t+w),-\mu+2(t-w)\Big),\quad \text{for } \mu>2w. \tag{13}$$

To verify the above mobility edges, we show the eigenenergy of the AA model with large quasi-periodic disorders in both the hopping and potential in Fig. 2(a). The parameters used are listed in the figure caption. Again, the color of each point represents the IPR value of the eigenstates. Similarly, we also plot the eigenenergy of the slowly varying AA model with the same disorders in Fig. 2(b). The values of the parameters of the slowly varying AA model are the same as those in the AA model with the large quasi-period, but with the varying exponent $v=0.5$. It can be seen from these figures that the mobility edges of the two types of models are both consistent with the calculated results of Eq. (13). In Figs. 2(c) and 2(d), the IPR values as a function of eigenenergy are shown for a few points with $\mu=0.9, 1.6, 2.5$. Whereas panel (c) shows the results of AA model with large quasi-period and panel (d) shows the results of slowly-varying AA model. It provides a more accurate verification of the mobility edges of Eq. (13).

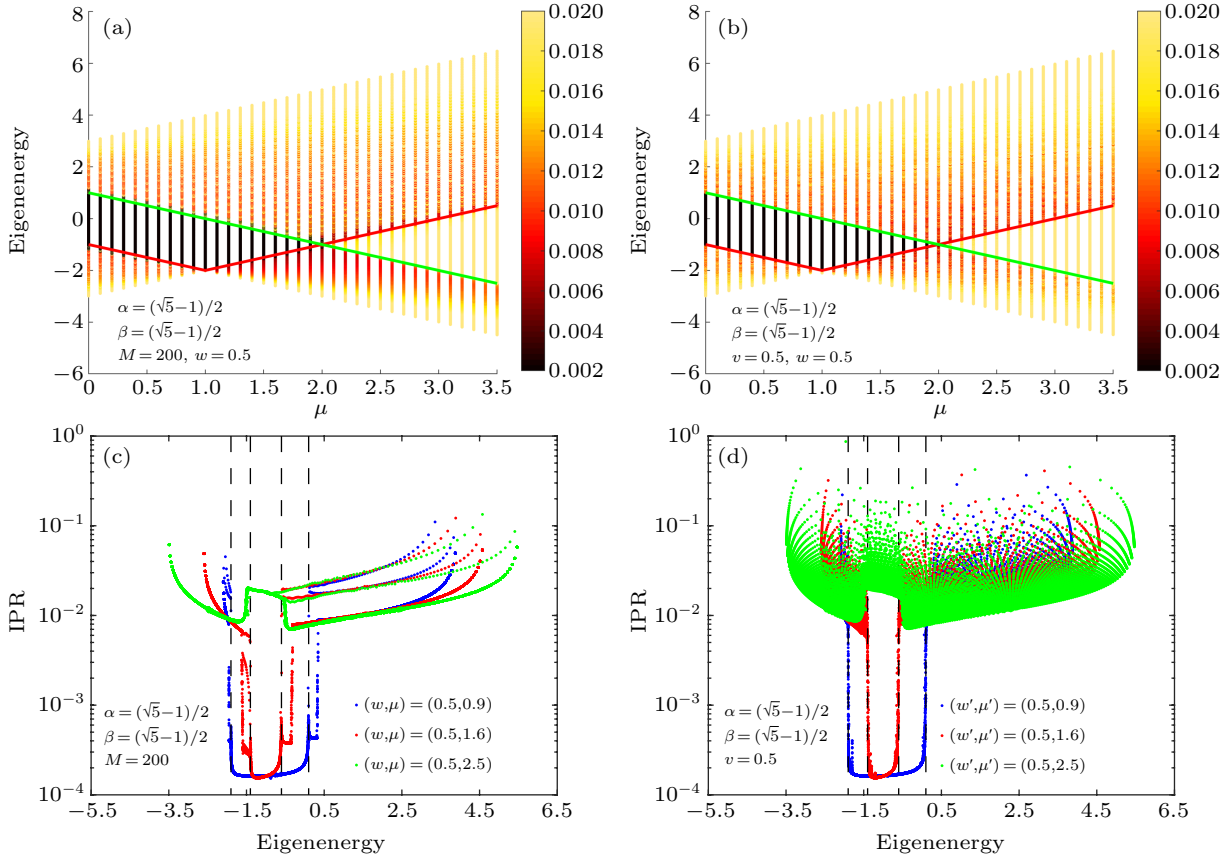


Fig. 2. (a) Eigenenergy of the AA model Eq. (1) as a function of μ with $\alpha=\beta=(\sqrt{5}-1)/2$, $w=0.5$ and $M=200$. (b) Eigenenergy of the slowly varying AA model Eq. (4) as a function of μ' with $w'=w$ and $v=0.5$, other parameters are the same as (a). The colors in panels (a) and (b) represent the IPR of each eigenstate. The red and green curves represent the mobility edges. (c) The IPR of the AA model as a function of eigenenergy for $(w,\mu)=(0.5,0.9)$, $(0.5,1.6)$, $(0.5,2.5)$, other parameters are the same as (a). (d) The IPR of the slowly varying AA model with $w'=w$ and $v=0.5$, where other parameters are the same as (c).

4.3. The AA model with different disorders in hopping and potential

As the last example, we consider the case with different disorders in hopping and potential. This can be easily achieved by setting $\phi\neq 0$. In this case, w_j and μ_j are not the same disorder, but they are also not completely independent. To determine the mobility edges, we still consider an ensemble of periodic models labeled by a with $w_a=w\cos(2\pi\alpha a/M)$ and $\mu_a=\mu\cos(2\pi\beta a/M-\pi/2)=\mu\sin(2\pi\beta a/M)$. Here we set the phase difference to be $\phi=-\pi/2$. Since in the periodic model H_a, w_a and μ_a are only constants, we can simplify the Eq. (8) to the following

$$E\in\bigcap_a\Big(R_{-a}-2t,R_{+a}+2t\Big), \tag{14}$$

here $R_{\pm a}$ is given by

$$R_{\pm a} = R\cos\left(\pm 2\pi\frac{\alpha}{M}a - \arctan\left(\frac{\mu}{2w}\right)\right),$$
$$R = \sqrt{\mu^2 + (2w)^2}. \tag{15}$$

For a given R, the smallest interval is given by taking $R_{-a} = R$ for lower bound and $R_{+a} = -R$ for upper bound. Therefore, we find that the overlap of all intervals, which is the region of extended states is given by

$$E \in \Big(R - 2t, -R + 2t\Big). \tag{16}$$

To verify the above mobility edges, we plot the eigenenergy of the above model with color indicating its IPR value in Fig. 3(a). The parameters are given in the figure caption. As a comparison, we also display the eigenenergy of the slowly varying AA model of Eq. (4) with the same type of disorders in Fig. 3(b). It can be seen from these figures that the mobility edges of the two types of models are consistent with the calculated results of Eq. (16). In Figs. 3(c) and 3(d), we show the IPR values as a function of eigenenergy for a few selective points of $\mu = 0, 1, 2$. The panels (c) and (d) correspond to the results of the AA model with large quasi-period and slowly-varying AA model, respectively. It provides more quantitative evidence that supports the mobility edges of Eq. (16).

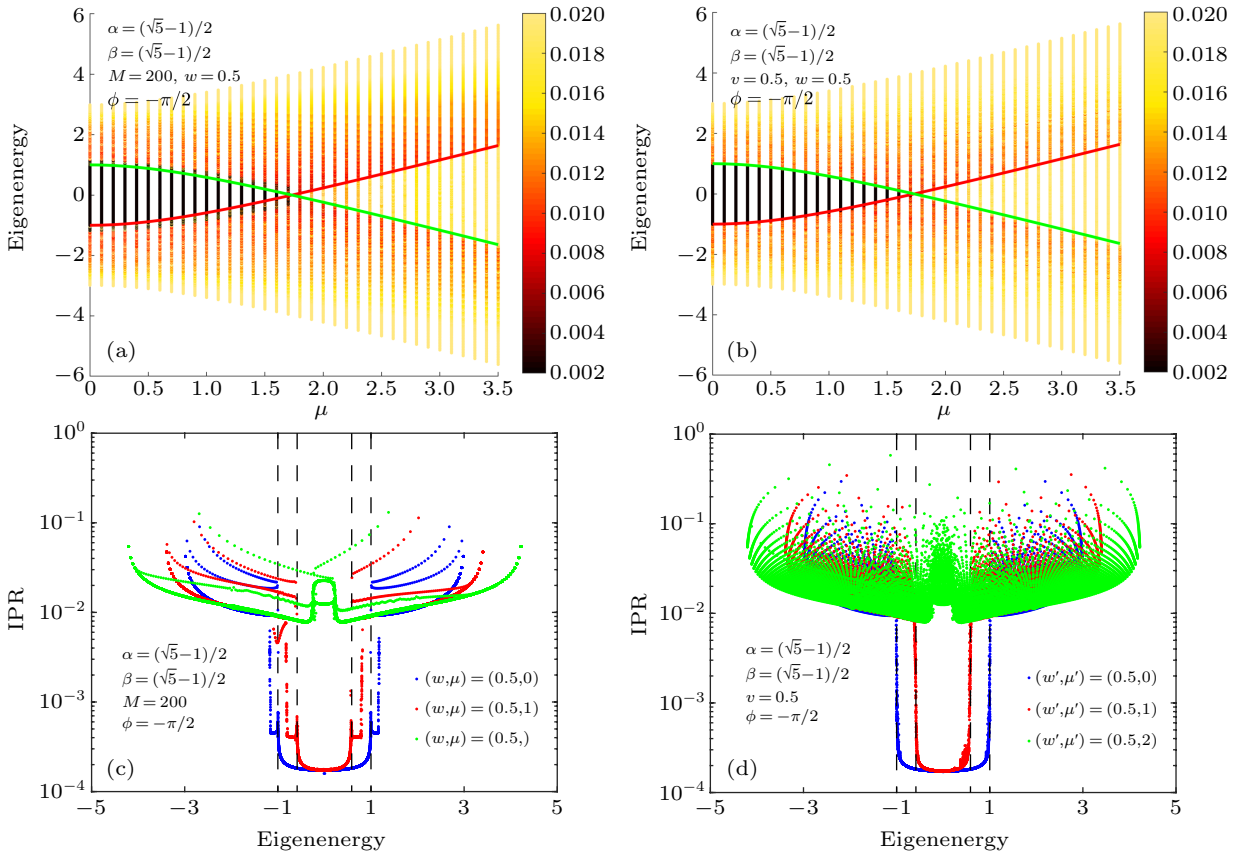


Fig. 3. (a) Eigenenergy of the AA model Eq. (1) as a function of μ with $\alpha = \beta = (\sqrt{5}-1)/2$, $w = 0.5$, $\phi = -\pi/2$ and $M = 200$. (b) Eigenenergy of slowly varying AA model Eq. (4) as a function of μ' with $w' = w$ and $v = 0.5$, other parameters are the same as (a). The colors in panels (a) and (b) represent the IPR of each eigenstate. The red and green curves represent the mobility edges. (c) The IPR of the AA model as a function of eigenenergy for $(w, \mu) = (0.5, 0), (0.5, 1), (0.5, 2)$, and other parameters are the same as (a). (d) The IPR of the slowly varying AA model with $w' = w$ and $v = 0.5$, and other parameters are the same as (c).

5. Qualitative explanations of the emergence of mobility edge with large quasi-period

In the original AA model, there is a duality point located at $\mu = 2t$. It has been proved rigorously[42] that the eigenstates are all localized for $\mu > 2t$ and are all extended for $\mu < 2t$. Because of this, no mobility edge exists for a fixed μ in the original AA model. Our modification of AA model is to make the irrational frequency very small as $\alpha \to \alpha/M$. The appearance of mobility edges in the large quasi-period models seems to contradict the above-mentioned theorem. We should emphasize that the observed mobility edges only show up for finite-sized systems. It is the combined effects of the large quasi-period and finite system size that make the mobility edge appear.

Here we want to show the effects of M on the model of Eq. (1). In Fig. 4, we plot the eigenenergy of the AA model of Eq. (1) with colors indicating its IPR value for several different M values. The parameters are given in the figure caption. In panel (a), we have $M = 1$ which is exactly the original AA model. One can clearly see that the duality point located at $\mu = 2$ separates the extended and localized states. Therefore,

for a fixed μ, there are no mobility edges. From panels (b) to (c), we gradually increase M from 60 to 120. Then for a fixed μ, there appear more and more localized states. But the location of the mobility edge is still not very clear. When we reach $M = 180$, the mobility edge becomes quite sharp and its location is the same as the mobility edge of the slowly varying disordered the AA model. These figures clearly show the relationship between the values of M and the appearance of mobility edges.

To see the effects of M more clearly, we propose another quantity that can reflect the degree of localization of each eigenstate. In the energy-matching method, we approximate the large quasi-period model by a lot of periodic models. For a given eigenenergy E, we can find the number of periodic models whose energy bands contain E. The eigenstates become more localized if this number becomes smaller. In Fig. 5, we plot the number of periodic models as a function of eigenerngy E for $\mu = 1.5$ and $\mu = 2.5$. For the left and right panels, $M = 50$ and 200, respectively. One can see that for $\mu = 1.5$, the number of periodic models rapidly decreases from the band center to the band edges. For larger M, this number decreases even faster. This indicates that the eigenstates near the band edges are essentially localized for $\mu < 2$.

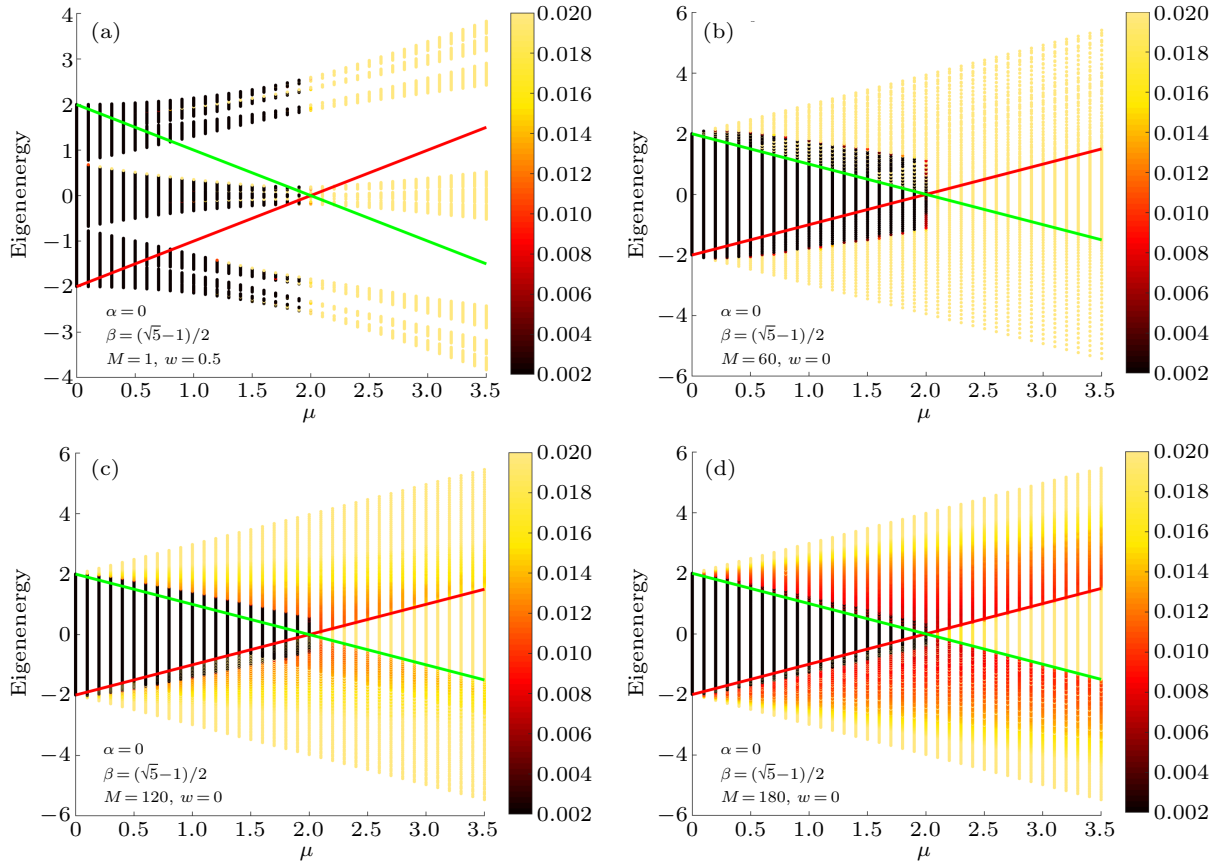


Fig. 4. Eigenenergy of the AA model Eq. (1) as a function of μ with $\alpha = 0$, $\beta = (\sqrt{5}-1)/2$, $w = 0$. The colors represent the IPR of each eigenstate. From (a) to (d), $M = 1$, 60, 120, 180, respectively.

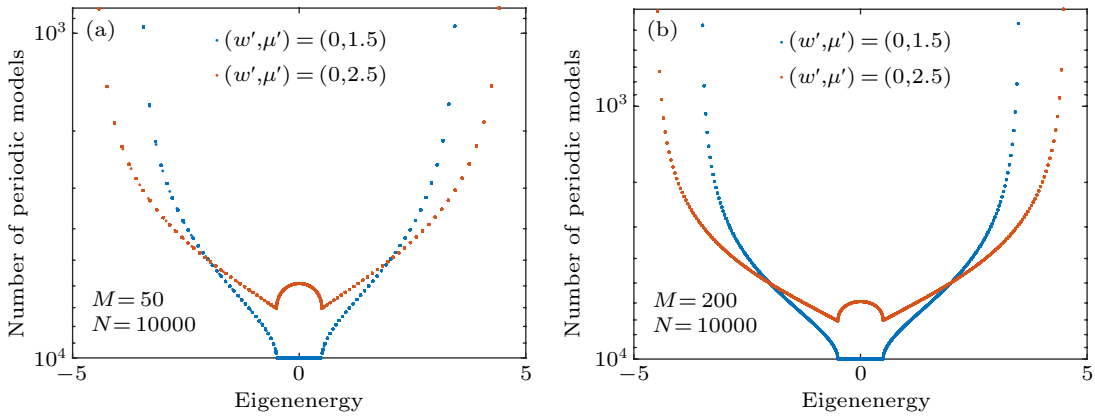


Fig. 5. The number of periodic models as a function of eigenenergy E for $\mu = 1.5$ (blue dots) and 2.5 (red dots). From left to right, $M = 50$, 200, respectively. Other parameters are $\alpha = 0$, $\beta = (\sqrt{5}-1)/2$, $M = 50$.

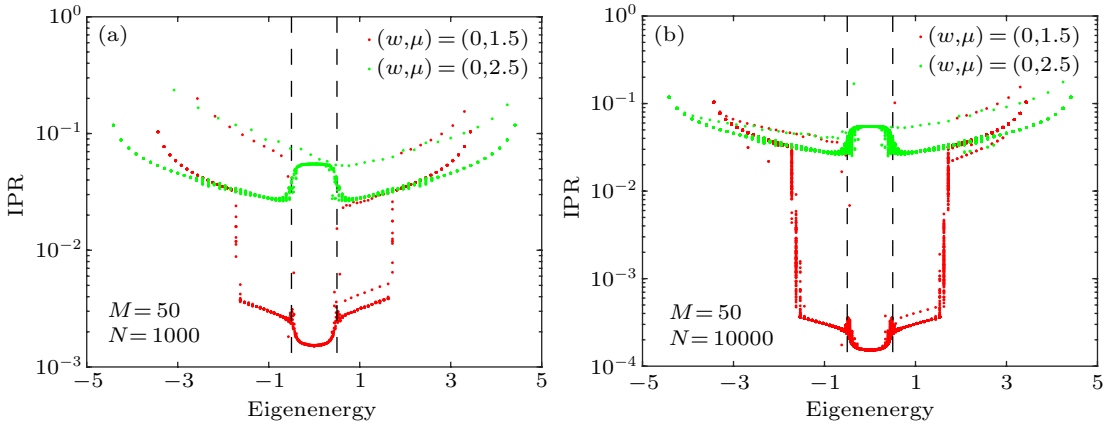


Fig. 6. The IPR value as a function of eigenenergy E for $\mu = 1.5$ (red dots) and 2.5 (green dots). From left to right, $N = 1000$, 10000, respectively. Other parameters are $\alpha = 0$, $\beta = (\sqrt{5}-1)/2$, $M = 50$.

The mobility edges of the AA model for a fixed μ are also observed in Ref. [43]. In this paper, it is argued that the original AA model can be thought as a 1D projection of the 2D Hofstadter model with incommensurate magnetic flux density. From this point of view, the localization of the eigenstate of the AA model near the band edge can be understood by semi-classical calculations of the 2D Hofstadter model with small magnetic flux density. We refer readers to Ref. [43] for more detailed explanations. These results are consistent with what we observed. In our paper, we also consider the generalized AA models and find similar results.

To see the effects of system size N, we plot the IPR value as a function of eigenenergy E for $N = 10^3$ and 10^4 in Fig. 6. Here the IPR is calculated for $\mu = 1.5$ and 2.5. The first μ is smaller than the critical $\mu_c = 2$ and the other is greater than it. One can see that if the system size is smaller, the IPR of states with these two μ become closer. One can also see that for fixed $\mu = 1.5$, the IPR also decreases a lot as one moves from the band edges to the band center. This shows there is some critical E for $\mu < 2$, which separates the extended and localized states. This feature is more observable for a finite-sized system. Because in this case, the IPR difference between $\mu < 2$ and $\mu > 2$ is not that large.

6. Conclusion

In this paper, we have shown that the AA-type model with the large quasi-period can also support mobility edges. By inserting the large quasi-periodic disorders in the hopping coefficients, the potentials or both, we demonstrate that the mobility edges in these examples are almost the same as the corresponding slowly varying disordered models. The precise locations of the mobility edges are deduced by the energy matching method. We argued that the appearance of mobility edges for a fixed μ in the large quasi-periodic disordered models is due to the combined effects of long quasi-period and finite system size. The longer quasi-period makes the IPR difference between the band edges and band center bigger. On the other hand, the smaller system size makes the IPR difference across the dual point smaller. Combining the above two effects, the mobility edges for a fixed μ become more apparent for a model with a large quasi-period and finite system size.

Acknowledgments

Project supported by the National Natural Science Foundation of China (Grant No. 11874272) and Science Specialty Program of Sichuan University (Grant No. 2020SCUNL210).

References

[1] Anderson P W 1958 *Phys. Rev.* **109** 1492
[2] Mott N 1887 *J. Phys. C: Solid State Phys.* **20** 3075
[3] Abrahams E, Anderson P W, Licciardello D C and Ramakrishnan T V 1979 *Phys. Rev. Lett.* **42** 673
[4] Lee P A and Ramakrishnan T V 1985 *Rev. Mod. Phys.* **57** 287
[5] Aubry S and Andre G 1980 *Ann. Israel Phys. Soc.* **3** 18
[6] Harper P G 1955 *Proc. Phys. Soc. A* **68** 874
[7] Das Sarma S, He S and Xie X C 1988 *Phys. Rev. Lett.* **61** 2144
[8] Das Sarma S, He S and Xie X C 1990 *Phys. Rev. B* **41** 5544
[9] Biddle J and Das Sarma S 2010 *Phys. Rev. Lett.* **104** 070601
[10] Hashimoto Y, Niizeki K and Okabe Y 1992 *J. Phys. A: Math. Gen.* **25** 5211
[11] Boers D J, Goedeke B, Hinrichs D and Holthaus M 2007 *Phys. Rev. A* **75** 063404
[12] Biddle J, Wang B, Priour D J and Das Sarma S 2009 *Phys. Rev. A* **80** 021603
[13] Lellouch S and Sanchez-Palencia L 2014 *Phys. Rev. A* **90** 061602
[14] Biddle J, Priour D J, Wang B and Das Sarma S 2011 *Phys. Rev. B* **83** 075105
[15] Li X P, Pixley J H, Deng D L, Ganeshan S and Das Sarma S 2016 *Phys. Rev. B* **93** 184204
[16] Li X, Li X P and Das Sarma S 2017 *Phys. Rev. B* **96** 085119
[17] Deng X, Ray S, Sinha S, Shlyapnikov G V and Santos L 2019 *Phys. Rev. Lett.* **123** 025301
[18] Saha M, Maiti S K and Purkayastha A 2019 *Phys. Rev. B* **100** 174201
[19] Wang Y C, Xia X, Zhang L, Yao H P, Chen X, You J G, Zhou Q and Liu X J 2020 *Phys. Rev. Lett.* **125** 196604
[20] Luschen H P, Scherg S, Kohlert T, Schreiber M, Bordia P, Li X, Das Sarma S and Bloch I 2018 *Phys. Rev. Lett.* **120** 160404
[21] Zhou L 2021 *Phys. Rev. Research* **3** 033184
[22] Huang K, Vu D, Li X and Das Sarma S 2020 *Phys. Rev. Lett.* **126** 106803
[23] Dwiputra D and Zen F P 2022 *Phys. Rev. B* **105** L081110
[24] Xu Z, Huangfu H, Zhang Y and Chen S 2022 *New J. Phys.* **22** 013036
[25] Yao H, Giamarchi T and Sanchez-Palencia L 2020 *Phys. Rev. Lett.* **125** 060401

[26] Roy S, Mishra T, Tanatar B and Basu S 2021 *Phys. Rev. Lett.* **126** 106803
[27] Liu T, Xia X, Longhi S and Sanchez-Palencia L 2022 *SciPost Phys.* **12** 027
[28] Goncalves M, Amorim B, Castro E V and Ribeiro P 2022 *SciPost Phys.* **13** 046
[29] Duthie A, Roy S and Logan D E 2021 *Phys. Rev. B* **103** L060201
[30] Nava A, Campagnano G, Sodano P and Giuliano D 2023 *Phys. Rev. B* **107** 035113
[31] Yuce C and Ramezani H 2022 *Phys. Rev. B* **106** 024202
[32] Liu T and Xia X 2022 *Phys. Rev. B* **105** 054201
[33] Han W and Zhou L 2022 *Phys. Rev. B* **105** 054204
[34] Chen W, Cheng S, Lin J, Asgari R and Gao X 2022 *Phys. Rev. B* **106** 144208
[35] Liu Y, Jiang X P, Cao J and Chen S 2020 *Phys. Rev. B* **101** 174205
[36] Cai X 2021 *Phys. Rev. B* **103** 214202
[37] Longhi S 2019 *Phys. Rev. B* **100** 125157
[38] Tang Q and He Y 2021 *J. Phys.: Condens. Matter* **33** 185505
[39] Thouless D J 1974 *Phys. Rep.* **13** 93
[40] Kohmoto M 1983 *Phys. Rev. Lett.* **51** 1198
[41] Schreiber M 1985 *J. Phys. C* **18** 2493
[42] Borgnia D S and Slager R J 2023 *Phys. Rev. B* **107** 085111
[43] Zhang Y, Bulmash D, Maharaj A V, Jian C M and Kivelson S A 2015 arXiv: 1504.05205